# Combined Near-Ambient Pressure Photoelectron Spectroscopy and Temporal Analysis of Products Study of CH<sub>4</sub> Oxidation on Pd/γ-Al<sub>2</sub>O<sub>3</sub> Catalysts

Joachim Pasel, <sup>1</sup>\* Dirk Schmitt, <sup>1</sup> Heinrich Hartmann, <sup>2</sup> Astrid Besmehn, <sup>2</sup> Jürgen Dornseiffer, <sup>3</sup>

Jonas Werner, <sup>4</sup> Joachim Mayer <sup>4</sup> and Ralf Peters <sup>1</sup>

<sup>1</sup>Institute of Energy and Climate Research, IEK-14: Electrochemical Process Engineering

<sup>2</sup>Central Institute of Engineering, Electronics and Analytics, ZEA-3: Analytics

<sup>3</sup>Institute of Energy and Climate Research, IEK-1: Materials Synthesis and Processing

Forschungszentrum Juelich GmbH, D-52425 Juelich, Germany

<sup>4</sup>Central Facility for Electron Microscopy (GFE), RWTH Aachen University, D-52074

Aachen, Gemany

Natural gas vehicles; CH<sub>4</sub> oxidation; Temporal analysis of products; Near-Ambient Pressure Photoelectron Spectroscopy; Pd active phases; Spill-over;

\* Corresponding author: Tel: +49 2461 615140; fax: +49 2461 616695; e-mail: j.pasel@fz-juelich.de

#### **Abstract**

Vehicles that run on natural gas must be equipped with an exhaust gas after-treatment system to burn their unavoidable CH<sub>4</sub> slip, which must not be released into the environment as CH<sub>4</sub> is a potent greenhouse gas. Pd is known as a highly active catalyst material for CH<sub>4</sub> oxidation. For this study, Pd was deposited on a  $\gamma$ -Al<sub>2</sub>O<sub>3</sub> support and the as-received samples were prereduced and pre-oxidized, respectively. Near-Ambient Pressure Photoelectron Spectroscopy and the Temporal Analysis of Products methodology were combined to understand that both

electronic states, namely PdO and Pd $^0$ , are active for the CH4 oxidation reaction, whereby the superior activity of the pre-reduced Pd $/\gamma$ -Al $_2$ O $_3$  catalyst was ascribed to the spill-over of OH-groups from the support to Pd. It was found that the reaction products, CO, CO $_2$  and H $_2$ , were strongly and, to a large extent, adsorbed on the catalyst surface and were involved in reversible chemical interactions on the catalyst surface during the CH4 oxidation reaction on the Pd $/\gamma$ -Al $_2$ O $_3$  catalyst.

#### Introduction

Natural gas with a high methane content (> 90%) is growing in public awareness as an alternative fuel to gasoline and diesel due to its low CO<sub>2</sub> emissions per energy content, low NOx emissions and its practical absence of particulate matter compared to other hydrocarbons. Furthermore, there is major future potential for producing CH<sub>4</sub> on a renewable basis by means of power-to-gas processes [1, 2]. However, as a greenhouse gas, the CH<sub>4</sub> slip being released by vehicles that run on natural gas must be treated catalytically [3] in an onboard exhaust gas after-treatment unit. The CH<sub>4</sub> slip amounts to roughly 5000 ppmv [4-6]. For the emissions control of methane-fueled engines, commercial Ce-Zr-promoted Pd-Rh/Al<sub>2</sub>O<sub>3</sub> catalysts (three way catalysts, TWCs), adapted from gasoline engines and designed for stoichiometric fuel to air mixtures ( $\lambda$ =1), are used [7]. However, the highest efficiency of natural gas engines can be reached under lean burn operation conditions with an excess of oxygen ( $\lambda$ >1). Accordingly, the periodically-oscillating lean/rich conditions, which are intrinsic to the operation of TWCs, consume additional fuel for effective CH<sub>4</sub> emission abatement and decrease the energetic efficiency. Previous studies by Tomposa et al. [8] and Huang et al. [9] show that both metal Pd<sup>0</sup> and its oxidized form, PdO, can function as active sites for CH<sub>4</sub> activation, whereby PdO is considered the prevailing active phase under oxidizing reaction conditions. It is also stated that an optimum ratio between metallic Pd and PdO species should be set to gain high activity. Kinnunen et al. [10] investigated the dissociation of the C-H bond in CH4 by means of DFT calculations and found that the coexistence of both phases, Pd<sup>0</sup> and PdO, is beneficial for the catalytic activity. Bounechada et al. [7] and Fouladvand et al. [11] describe Pd<sup>0</sup> as only being stable under dynamic oscillating conditions around  $\lambda=1$  (change from lean to rich reaction conditions and vice versa) of a gasoline motor and oxidizing to less active, pure PdO particles when switching to the lean burn operation conditions of the engine. As a consequence, the light-off for CH<sub>4</sub> oxidation shifts to higher temperatures, resulting in increasing CH<sub>4</sub> emissions. Against this background, the stabilization of the optimum ratio between metallic Pd and PdO in the exhaust catalyst is a fundamental requirement for establishing highly efficient, lean-burned, natural gas-fired engines.

For an improved understanding of the role of metallic Pd<sup>0</sup> and PdO during catalytic CH<sub>4</sub> oxidation, transient studies of the physico-chemical interaction between CH<sub>4</sub>, the possible reaction products, CO, CO<sub>2</sub>, H<sub>2</sub>, H<sub>2</sub>O, and the catalytic surface of a Pd/γ-Al<sub>2</sub>O<sub>3</sub> catalyst using

the Temporal Analysis of Products (TAP) methodology, were carried out in this study. The catalyst was exposed to oxidative and reductive pretreatments, generating well-defined and reproducible electronic states of the Pd species on the catalyst surface prior to its experimental TAP evaluation for CH<sub>4</sub> oxidation. Near-Ambient Pressure Photoelectron Spectroscopy (NAP-XPS) was applied to determine the electronic states of the Pd species following the respective pretreatments and to work out explanatory approaches for potentially different catalytic behaviors. The used Pd/γ-Al<sub>2</sub>O<sub>3</sub> catalyst was synthesized via a colloidal impregnation technique and characterized by N<sub>2</sub> sorption, as well as by Transmission Electron Microscopy (TEM), to determine the particle size of the Pd species. The Pd loading was restricted to 5 wt.%, as is described by Seeburg at al. [4], where higher loadings did not result in significantly improved catalytic activities.

# **Experimental**

## Preparation of the Pd/ $\gamma$ -Al<sub>2</sub>O<sub>3</sub> catalyst

The supported Pd catalyst on  $\gamma$ -Al<sub>2</sub>O<sub>3</sub> (Puralox TH 100/150 L4, Sasol, Hamburg Germany) was prepared using a colloid adsorption method. In order to be able to observe the changes in the oxidation state of the Pd particles by NAP-XPS in high resolution, the precious metal content was determined as 5 wt.% Pd. For the synthesis of 10 g of the catalyst, 1.22 g of Pd(NO<sub>3</sub>)<sub>2</sub> hydrate (Pd content 41 wt.-%, Alfa Aesar) and 1.2 g polyvinylpyrrolidone (K15, Sigma Aldrich) were first dissolved in 100 ml of water and 100 ml of methanol was rapidly added with vigorous stirring. The reaction mixture was then heated under reflux for 0.5 h to complete the colloid generation [12]. In the resulting deep black dispersion, 9.5 g of the  $\gamma$ -Al<sub>2</sub>O<sub>3</sub> support was rapidly added. After stirring overnight at room temperature, the obtained black powder was separated from the water as a clear solvent by filtration, thoroughly washed with distilled water, dried overnight at 120 °C and calcined for 2 h in air at a temperature of 550 °C.

# Catalyst synthesis and characterization (N<sub>2</sub> sorption and TEM)

The specific surface areas (SSA) of the Pd/ $\gamma$ -Al<sub>2</sub>O<sub>3</sub> catalyst and the  $\gamma$ -Al<sub>2</sub>O<sub>3</sub> support were measured by N<sub>2</sub> adsorption at liquid N<sub>2</sub> temperature using the Micrometricis Gemini 2360 system. In order to remove any residual water from the surface, the samples were pretreated overnight at 200 °C under flowing He prior to adsorption. The surface area was then determined using the standard Brunauer-Emmet-Teller (BET) method [13]. Subsequently, the pore size distribution was calculated from the obtained adsorption isotherms in the range of p/p<sub>0</sub> = 0.05-0.95 in accordance with the Cranston-Inclay methodology [14].

To determine the size distribution of the Pd particle on the γ-Al<sub>2</sub>O<sub>3</sub> support, Transmission Electron Microscopy (TEM) measurements were carried out using a 200 kV LIBRA 200FE (Carl Zeiss Microscopy GmbH, Oberkochen, Germany) equipped with a high-angle annular

dark-field (HAADF) detector (E.A. Fischione Instruments, Inc., Export, PA, USA), an energy-dispersive X-ray spectroscopy (EDX) apparatus (Bruker AXS GmbH, Karlsruhe, Germany) and a charge-coupled device (CCD) camera (Gatan, Inc., Pleasanton, CA, USA). TEM measurements were performed on the Pd/γ-Al<sub>2</sub>O<sub>3</sub> catalyst and the Al<sub>2</sub>O<sub>3</sub> support as a powder, which was dispersed in VE water using an ultrasonic bath and brought onto a carbon-coated copper TEM grid.

#### **NAP-XPS**

XP spectra were recorded at room temperature on a Specs NAP-XPS system equipped with a  $\mu$ -FOCUS 600 X-ray monochromator, an XR 50 MF X-Ray source and a PHOIBOS 150 NAP analyzer before and after the respective catalyst pre-treatments. The Al K $\alpha$  X-ray source (1486.6 eV) was operated at 50 W with a 15 kV anode voltage. The instrument is equipped with an in-situ reaction cell, which allows gas pressures of up to 20 mbar. In order to minimize the charging of the sample, the measurements were performed at 2 mbar Ar. The binding energies of the spectra were referenced to the Al 2p peak at 74.1 eV [15]. The oxidative catalyst pre-treatment was performed with pure O<sub>2</sub> at a pressure of 10 mbar at 400 °C, while the reductive pre-treatment was performed with a mixture of 2.5 mole% H<sub>2</sub> in Ar at a pressure of 10 mbar at 400 °C. The heating of the sample was performed by an IR laser against the backside of the sample holder, with the temperature controlled by a type K thermocouple mounted on the surface of the sample.

### **TAP**

For the TAP experiments, a commercial TAP-KPC reactor system (Mithra Technologies, Inc.) was applied, which can be operated in two different modes. In the commonly called "transient mode", small gas pulses with pulse widths of between 90-130  $\mu$ s were injected into the TAP micro-reactor at ultra-high vacuum conditions, whereas the so-called "flow mode" operates at atmospheric pressure with a constant flow of specific gases for, e.g., pre-treatment purposes. For each experiment, 20 mg of the Pd/ $\gamma$ -Al<sub>2</sub>O<sub>3</sub> catalyst with particle sizes between 200  $\mu$ m and 400  $\mu$ m were filled into the TAP micro-reactor. For a kinetic experiment using the TAP methodology, three major requirements must be fulfilled from an experimental point of view [16-21]:

• The transport of gases through the catalyst sample is well-defined and only happens as a result of Knudsen diffusion. Gas molecules more likely hit the reactor wall or interact with the catalyst rather than react with one another. Thus, gas phase reactions can be suppressed. As a result, any deviation of the TAP response pulses (e.g., broader or narrower pulses) in comparison to the only Knudsen diffusion case (e.g., using Ar as the internal standard) can be ascribed to the chemical interactions of the respective gas molecules with the catalyst and help shed light on the overall reaction network.

- The active catalytic material is only allowed to slightly change from one inlet pulse to the next ("temporal uniformity"). Such an experiment is considered to be "state-defining". This means that, experimentally, the number of molecules contained in one inlet pulse is small compared to the number of accessible active sites on the catalyst.
- The third requirement is the "spatial uniformity" of the catalytically-active material. Here, the state of the catalyst, characterized by its surface coverages, must remain uniform within each pulse. By establishing a so-called "thin-zone reactor" concept for which the ratio of the thickness of the catalyst bed to the length of the TAP microreactor is in the range of 1/10 to 1/30, the changes to the surface coverages across the catalyst bed are small in comparison to their absolute values.

The "thin-zone reactor" concept was realized by utilizing a catalyst bed with a length of approximately 1 mm, while the total length of the TAP micro-reactor was approximately 34 mm. Hereby, the porosity of the catalyst bed was estimated to be 0.45. Furthermore, by limiting the number of moles of CH<sub>4</sub> per inlet pulse during all experiments to 2-3 \*10<sup>-9</sup>, the above-mentioned prerequisite of a "state-defining" experiment can be considered fulfilled.

For all TAP experiments in this paper in the transient mode in which CH<sub>4</sub> was involved, the inlet pulses contained 5 mole% CH<sub>4</sub> in Ar. No O<sub>2</sub> was added. The reaction temperature was varied between 100 °C and 500 °C in 50 K intervals. Experiments regarding the single adsorption and desorption of the reaction products CO<sub>2</sub>, CO and H<sub>2</sub>, respectively, on the Pd/γ-Al<sub>2</sub>O<sub>3</sub> catalyst, were also performed in the transient mode with mixtures of 5 mole% of the respective gases in Ar. The above-mentioned reductive pre-treatment, prior to injecting the CH<sub>4</sub>-containing pulses onto the catalyst surface, was performed at atmospheric pressure in the flow mode using a mixture of 2.5 mole% H<sub>2</sub> in Ar at 400 °C for 22 h or pure CH<sub>4</sub> at 400 °C for 20 h, respectively. For the oxidative pre-treatment, pure O<sub>2</sub> at 400 °C for 22 h was fed through the catalyst bed. The pulse responses for CH<sub>4</sub>, CO, CO<sub>2</sub>, H<sub>2</sub>, H<sub>2</sub>O and Ar were recorded with a mass spectrometer (Stanford Research Systems RGA 200) at m/z values of 16, 28, 44, 2, 18 and 40, respectively.

#### Results and discussion

## Catalyst characterization (N<sub>2</sub> sorption and TEM)

Utilizing Transmission Electron Microscopy, the morphologies of the support and the PdO nanoparticles of the as-received Pd/ $\gamma$ -Al<sub>2</sub>O<sub>3</sub> catalyst after calcination in air at 550 °C were identified. Figure 1 shows the TEM image (left) of the supported Pd/ $\gamma$ -Al<sub>2</sub>O<sub>3</sub> catalyst, which was formed from Al<sub>2</sub>O<sub>3</sub> particles with irregular shapes in the range of 15-30 nm. On this  $\gamma$ -Al<sub>2</sub>O<sub>3</sub> surface, spherical PdO particles in a size range between 3 and 8 nm were observed (Figure 1, on the right), which are statistically distributed within the pores of the catalyst with a slight tendency towards clustering. The PdO nanoparticles were identified with HAADF-STEM images for the fact that the influence of heavier elements on the image contrast is

stronger, i.e., particles formed by elements with higher atomic numbers appear brighter. In addition, Figure 2 shows, on the left-hand side, a magnified HAADF-STEM image of the  $Pd/\gamma$ -Al<sub>2</sub>O<sub>3</sub> catalyst with an individual, bright particle (tagged with the reticule), whose EDX findings are shown on the right-hand side of the figure. They confirm the presence of O, Al and Pd on the catalyst surface. The measured Cu signal originates from the sample grid material.

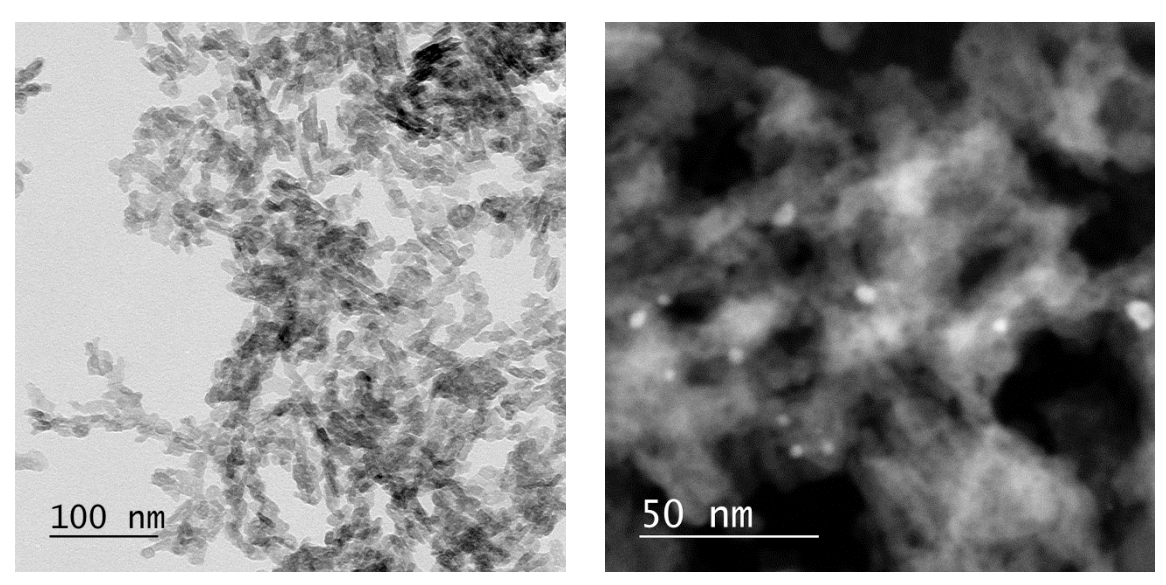


Figure 1 TEM image of the 5 wt.% Pd/γ-Al<sub>2</sub>O<sub>3</sub> catalyst (left) and HAADF-STEM image of the PdO nanoparticles inside the pores (right)

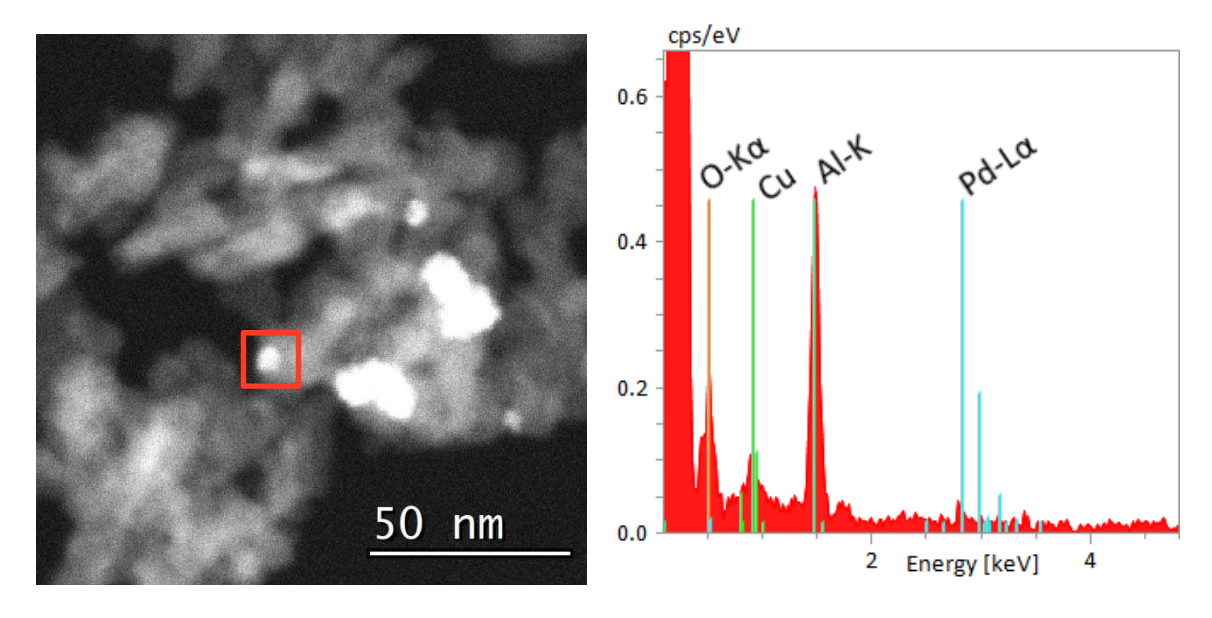


Figure 2 Magnified HAADF-STEM image of the Pd/γ-Al<sub>2</sub>O<sub>3</sub> catalyst (left) with corresponding qualitative EDX findings (right)

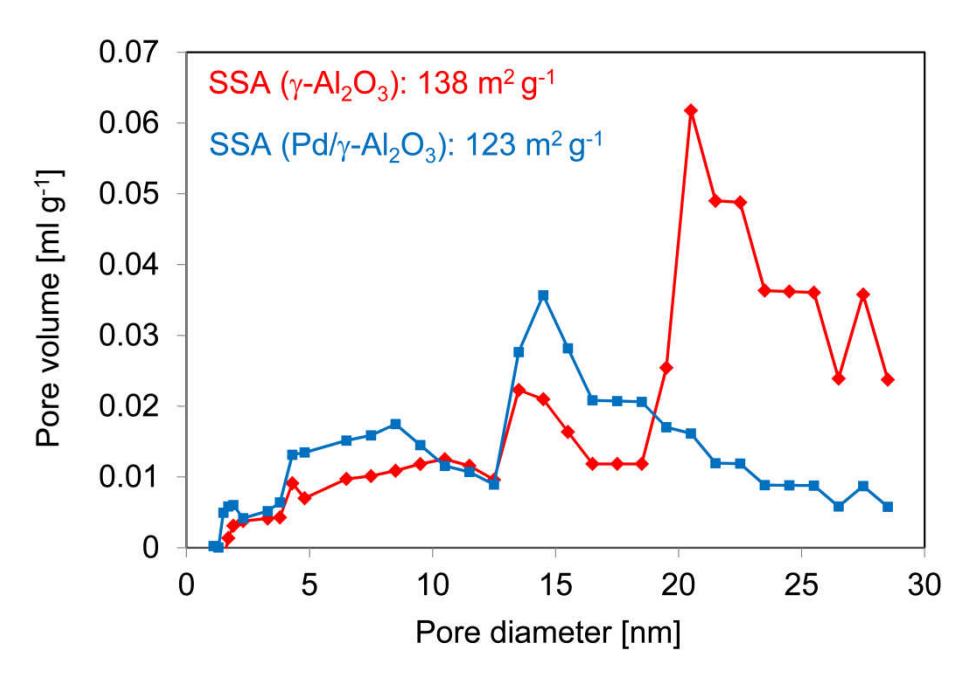


Figure 3 Specific surface areas and pore size distributions of the γ-Al<sub>2</sub>O<sub>3</sub> support and the 5 wt.% Pd/γ-Al<sub>2</sub>O<sub>3</sub> catalyst after coating with Pd

The pore size distributions of the  $\gamma$ -Al<sub>2</sub>O<sub>3</sub> support and the 5 wt.% Pd/ $\gamma$ -Al<sub>2</sub>O<sub>3</sub> catalyst in Figure 3 reveal that, after precious metal coating, the average pore diameter of the uncoated  $\gamma$ -Al<sub>2</sub>O<sub>3</sub> decreased from 22 nm to 15 nm due to the high Pd loading of 5 wt.-%. In addition, a larger amount of smaller pores in the range between 5 nm and 10 nm were formed in the case of the Pd/ $\gamma$ -Al<sub>2</sub>O<sub>3</sub> catalyst, resulting in a total specific surface area of 123 m<sup>2</sup> g<sup>-1</sup>, which was only 15 m<sup>2</sup> g<sup>-1</sup> lower than that of the uncoated support.

#### **NAP-XPS**

Figure 4 shows the Pd 3d spectrum of the pre-reduced Pd/ $\gamma$ -Al<sub>2</sub>O<sub>3</sub> catalyst (a); and after the oxidative pre-treatment for 2 h (b); and 4 h (c) in accordance with the oxidative pre-treatment procedure described above. Part (a) of Figure 4 shows two asymmetric peaks at 334.8 eV and 340.0 eV, which make up the 3d doublet of metallic Pd<sup>0</sup> [22-24]. However, already after two hours of oxidative pre-treatment at 400 °C, two additional major peaks appeared at 336.7 eV and 342.0 eV that can be assigned to Pd(II) [24, 25]. The two smaller peaks at 339.6 eV and 344.9 eV are shake-up features that belong to the main oxide species [26]. After a total of four hours with oxidative pre-treatment, the spectrum only shows the peaks belonging to the oxidized Pd species, indicating that the Pd<sup>0</sup> particles are fully oxidized within the sampling depth of 5-10 nm.

Figure 5 displays the Pd 3d spectrum of an almost fully oxidized Pd/γ-Al<sub>2</sub>O<sub>3</sub> catalyst (a); and after the reductive pre-treatment for 2 h (b) as per the reductive pre-treatment procedure described above. The Pd 3d spectrum of the catalyst in part (b) of this figure only shows the two asymmetric peaks that belong to metallic Pd<sup>0</sup>, indicating that the Pd particles undergo a complete reduction within the sampling depth of 5-10 nm under these reductive conditions. Furthermore, the Al 2p and O 1s regions of the oxidized and reduced catalysts do not display

any changes that could be attributed to the presence of OH-groups on the catalyst surface after the reductive pre-treatment.

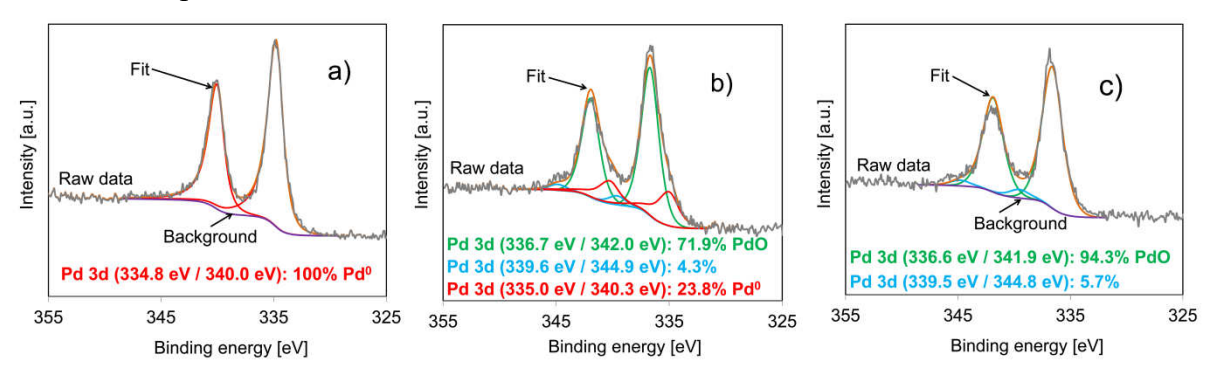


Figure 4 Pd 3d spectrum of the pre-reduced Pd/γ-Al<sub>2</sub>O<sub>3</sub> catalyst (a); and Pd 3d spectra after the oxidative pre-treatment for 2 h (b); and 4 h (c) in accordance with the oxidative pre-treatment procedure described above

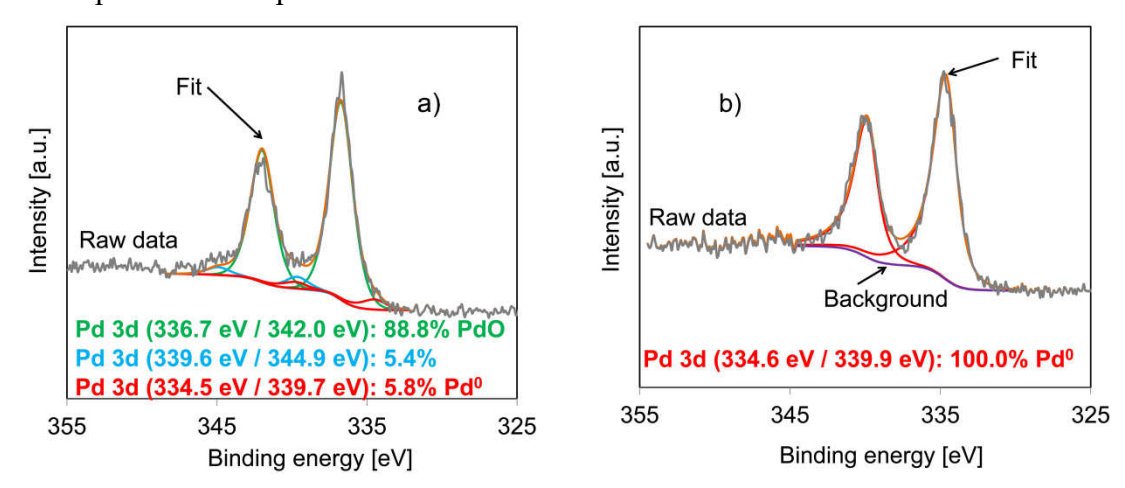


Figure 5 Pd 3d spectrum of an almost fully oxidized Pd/γ-Al<sub>2</sub>O<sub>3</sub> catalyst (a); and Pd 3d spectrum after the reductive pre-treatment for 2 h (b) as per the reductive pre-treatment procedure described above

The results from these figures indicate that the oxidative and reductive pre-treatments, as they are described in the experimental section, were highly effective with respect to the formation of the desired well-defined PdO- and Pd<sup>0</sup>-phases, respectively, prior to injecting the CH<sub>4</sub>-containing pulses in the TAP experiments.

# **Temporal Analysis of Products**

The experiments displayed in Figure 6 aim to shed light on the adsorption and desorption behavior of the reaction products, CO, CO<sub>2</sub> and H<sub>2</sub>, possibly formed in the following reaction equations.

$$CH_4 + 2 O_2 \iff CO_2 + 2 H_2 O$$
 exothermic (1)  
 $CH_4 + 1/2 O_2 \iff CO + 2 H_2$  exothermic (2)  
 $CH_4 \iff 2 H_2 + C$  endothermic (3)

Prior to these experiments, the catalyst was exposed to Ar in flow mode at 400 °C for 30 min. All displayed response pulses of CO, CO<sub>2</sub> and H<sub>2</sub> in Figure 6 were normalized to the Ar signal by multiplying the recorded raw outlet intensities of CO, CO<sub>2</sub> and H<sub>2</sub>, respectively, by the ratio of the maximum Ar outlet intensity recorded on inert quartz to the maximum Ar outlet intensity recorded on the Pd/γ-Al<sub>2</sub>O<sub>3</sub> catalyst. Furthermore, for the quantification of the percentages of desorbed CO, CO<sub>2</sub> and H<sub>2</sub> molecules as given in Figure 6, not only the zeroth moments of CO, CO<sub>2</sub> and H<sub>2</sub>, but also those of the corresponding Ar response pulses were considered.

In the top part, Figure 6 shows, on the left-hand side (a) the response pulses for CO during single adsorption on inert quartz (one average signal calculated from several hundred pulses) and, on the Pd/γ-Al<sub>2</sub>O<sub>3</sub> catalyst (one average signal calculated from a series of subsequent 15 pulses) at 200 °C, respectively, after a mixture of 5 mole% CO in Ar has been injected onto the respective samples in transient mode. On the right-hand side (b), the respective results at 400 °C are shown. It becomes evident that at both temperatures, 200 °C and 400 °C, the response pulses for CO on the Pd/γ-Al<sub>2</sub>O<sub>3</sub> catalyst were much smaller than those on inert quartz. Quantitatively, at both temperatures, only about 16-17% of the injected molecules could be detected at the outlet of the reactor. This means that CO is adsorbed strongly and, to a large extent, on the Pd/γ-Al<sub>2</sub>O<sub>3</sub> catalyst, almost independent of the temperature. These results stand in contrast to those obtained by Kuhn et al. [27] who found CO desorption from differently annealed Pd (111) surfaces at temperatures lower than 275 °C with maxima at approximately 225 °C However, reproduction experiments could confirm the findings from Figure 6 and also proved that at both temperatures, 200 °C and 400 °C, no CO<sub>2</sub> was produced.

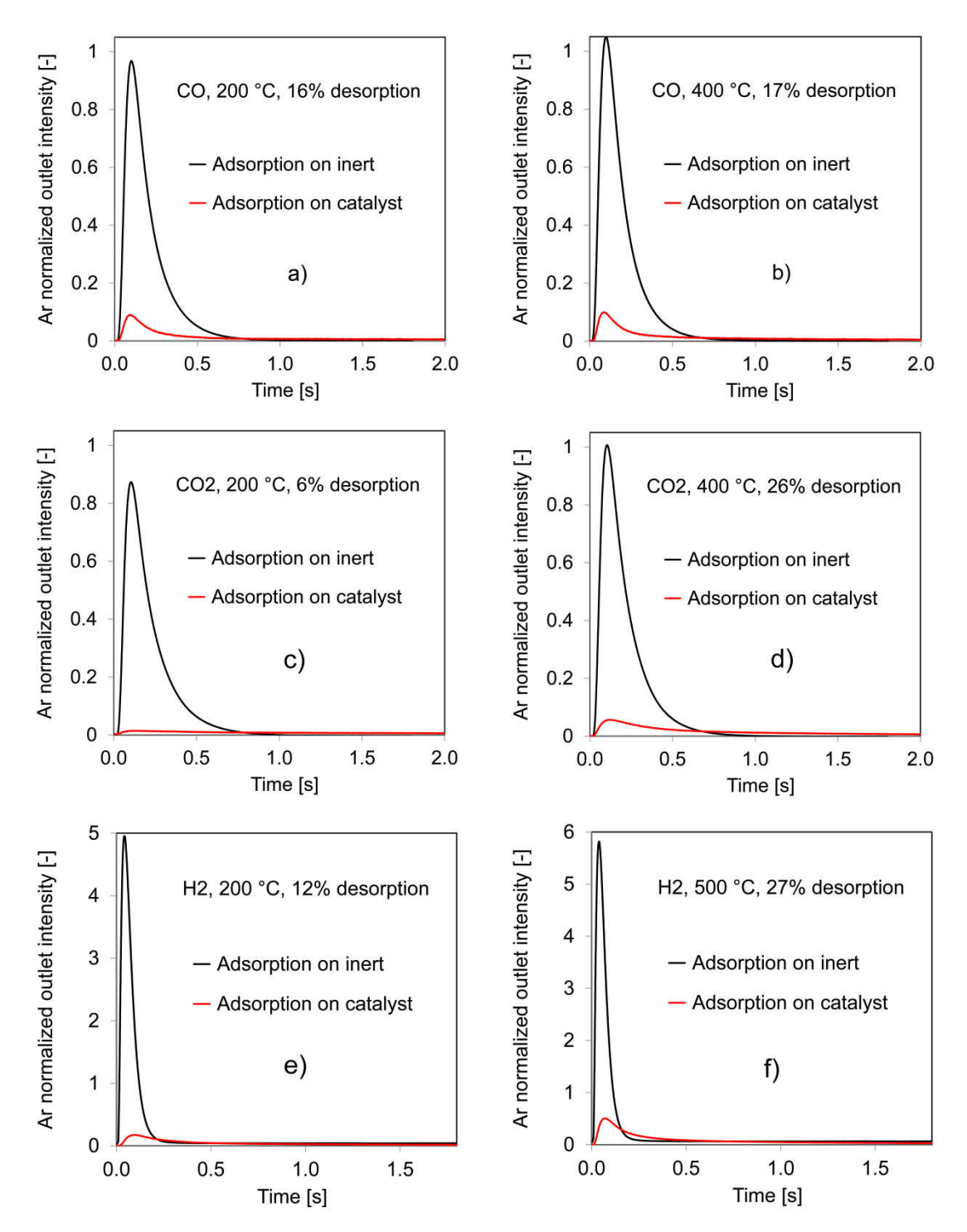


Figure 6 Response pulses in transient mode during single adsorption on inert quartz and the Pd/γ-Al<sub>2</sub>O<sub>3</sub> catalyst for CO at 200 °C (a) and 400 °C (b) from a mixture of 5 mole% CO in Ar, for CO<sub>2</sub> at 200 °C (c) and 400 °C (d) from a mixture of 5 mole% CO<sub>2</sub> in Ar and for H<sub>2</sub> at 200 °C (e), and 500 °C (f) from a mixture of 5 mole% H<sub>2</sub> in Ar

Similar pictures emerge in Figure 6, where the same single adsorption experiments described above were performed with CO<sub>2</sub> (cf. figures (c) and (d)) at 200 ° and 400 °C, respectively, and with H<sub>2</sub> (cf. figures (e) and (f)) at 200 ° and 500 °C, respectively. Also, CO<sub>2</sub> and H<sub>2</sub> adsorbed strongly and, to a large extent, on the surface of the Pd/ $\gamma$ -Al<sub>2</sub>O<sub>3</sub> catalyst. However,

in the case of CO<sub>2</sub> and H<sub>2</sub>, a slight temperature effect was observed, leading to stronger desorption from the catalyst surface at 400 °C and 500 °C, respectively. Also in these cases, reproduction experiments could confirm the described findings. They also showed that during the single H<sub>2</sub> adsorption experiments, no H<sub>2</sub>O could be detected in the outlet of the microreactor by means of mass spectrometry.

The TAP product response pulses in time can be regarded as a residence time distribution in a plug flow reactor. Comparing them qualitatively can yield helpful information about the structure of the entire reaction network. On the one hand, in many cases reaction products involved in reversible processes on the catalyst surface show up later at the exit of the TAP micro-reactor in comparison to residual educts or inert components such as Ar, as they must overcome some kinetic resistance on their way, e.g., the adsorption time scale of the pristine reactant, as well as that of the reaction itself, plus that of their desorption from the surface. These reversible processes lead to a broadening of the response pulses in comparison to the diffusion-only case with Ar. On the other hand, however, if the probability of reacting for educt molecules is different from zero, those educt molecules with a stochastically longer residence time will be more likely to react, whereas those molecules that are able to pass the catalyst bed faster have a far better chance of overcoming the traverse across the catalyst bed. As a consequence, the resulting response pulse for molecules undergoing irreversible processes on the catalyst surface is narrowed in comparison to the diffusion-only case with Ar. With respect to the experiments reported in this paper, Figure 7 presents the normalized outlet intensities as a function of the mass corrected time of CH<sub>4</sub>, CO and Ar at temperatures of 100 °C, 150 °C and 250 °C, respectively, on the H<sub>2</sub> pre-reduced Pd/γ-Al<sub>2</sub>O<sub>3</sub> catalyst after a mixture of 5 mole% CH<sub>4</sub> in Ar was injected in transient mode. The normalization of the outlet intensities of the pulses to the same height was performed by simply dividing the values of each curve by its peak value. The mass correction of the time of all response pulses was performed by multiplying the experimentally-recorded time values with the square root of (M<sub>Ar</sub>/M<sub>gas</sub>). Here, M<sub>Ar</sub> stands for the molar mass of Ar and M<sub>gas</sub> for that of the other gases dealt with in Figure 7. In the CH<sub>4</sub> case, for instance, the recorded time values were multiplied by the square root of (40/16). This mathematical procedure emphasizes how much the different gases are delayed or expedited from their expected values in the diffusion-only case with Ar. It becomes obvious from Figure 7 that, apart from Ar as internal standard and unreacted CH<sub>4</sub>, CO formed as per reaction equation (2) was the only product that could be detected in the outlet flow of the TAP micro-reactor at temperatures between 100 °C and 250 °C. Other possible reaction products, such as of H<sub>2</sub>, CO<sub>2</sub> or H<sub>2</sub>O, were not formed at all or strongly stuck to the γ-Al<sub>2</sub>O<sub>3</sub> support under the TAP reaction conditions. CH<sub>4</sub> conversions were significantly high, amounting to 25-50% at these comparatively low reaction temperatures. In Figure 7, in any case the response pulses of CO and unreacted CH<sub>4</sub> were plainly broader than those of Ar. It can be qualitatively concluded from these results that both the molecules, CO and CH<sub>4</sub>, were involved in reversible chemical interactions like adsorption

and desorption on the catalyst surface. It is remarkable that at all temperatures between 100-250 °C, the response pulses of CO and CH<sub>4</sub> initially showed a coincident rising part which indicates that at shorter residence times (up to approximately 0.09 s) the desorption of generated CO and unreacted CH<sub>4</sub> molecules took place simultaneously. This finding means that for these cases, the multiple surface steps leading from CH4 to CO (several C-H bond cleavages and a C-O bond formation) were very fast in comparison with the CH<sub>4</sub> desorption itself and, moreover, in comparison with other slower steps that control the profound tailing of the CO and CH<sub>4</sub> response pulses compared to the diffusion-only case with Ar at residence times longer than 0.09 s. It is interesting to note that, at 100 °C and 150 °C, the tailings of the response pulses of CH<sub>4</sub> were broader than those of CO in the time span from approximately 0.09-0.50 s, while at 250 °C, the curves for CO and CH4 were very similar also across the time span of the tailing. It can be concluded that in the tailing parts of the respective response pulses, the reversible chemical interactions of CH<sub>4</sub> on the catalyst surface were more complex at low temperatures and low CH<sub>4</sub> conversions (approximately 25%) and became comparable with respect to their extent to those of CO at 250 °C and CH<sub>4</sub> conversions in the range of 50%. Furthermore, in Figure 7, there are temperature-dependent crossing points between the response pulses of CO and CH4. At 100 °C, the crossing point was at 0.58 s and shifted to 0.41 s at 250 °C. The position of the crossing point is influenced by the number of steps on the surface and the complexity of the reaction network, and is also affected by the magnitude of the rate constants. The exact origin of the relative shape changes as a function of the temperature between CO and CH<sub>4</sub> is beyond the scope of analysis without modeling of the transients. However, the modeling of the transients is not carried out in this paper. The abovementioned finding, that the response pulses of CH4 were broader than those of Ar for the diffusion-only case, stands in contrast to the findings of Dhainaut et al. [28], who detected a narrower TAP response pulse for CH<sub>4</sub> compared to that of Ar on their Pd/Al<sub>2</sub>O<sub>3</sub> catalyst (2.5 wt% Pd), indicating irreversible processes on the catalyst surface in this case.

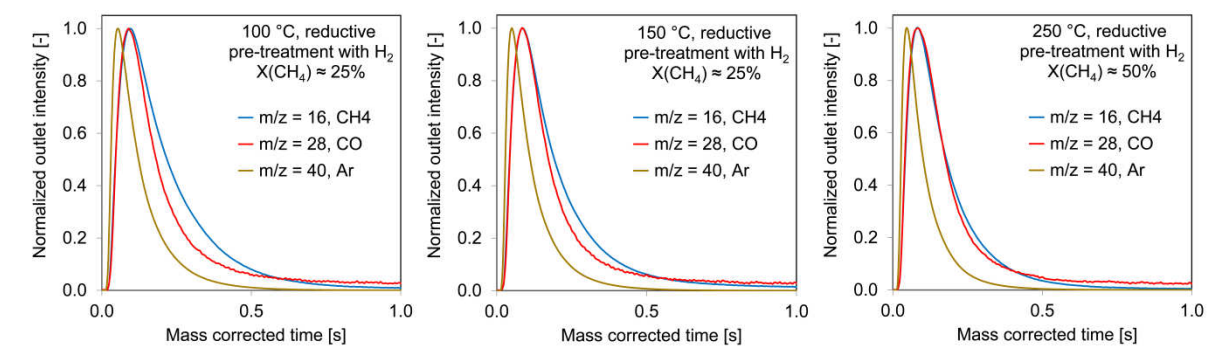


Figure 7 Normalized outlet intensities in transient mode as a function of the mass corrected time of CH<sub>4</sub>, CO and Ar at temperatures of 100 °C, 150 °C and 250 °C, respectively, on the H<sub>2</sub> pre-reduced Pd/γ-Al<sub>2</sub>O<sub>3</sub> catalyst from a mixture of 5 mole% CH<sub>4</sub> in Ar

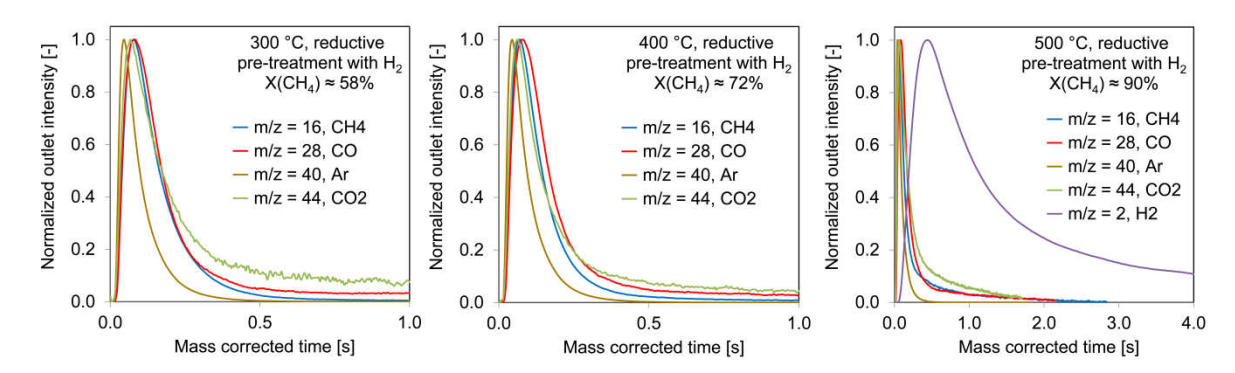


Figure 8 Normalized outlet intensities in transient mode as a function of the mass corrected time of CH<sub>4</sub>, CO, CO<sub>2</sub>, H<sub>2</sub> and Ar at temperatures of 300 °C, 400 °C and 500 °C, respectively, on the H<sub>2</sub> pre-reduced Pd/ $\gamma$ -Al<sub>2</sub>O<sub>3</sub> catalyst from a mixture of 5 mole% CH<sub>4</sub> in Ar

As a continuation of the experiments shown in Figure 7, Figure 8 presents the normalized outlet intensities in transient mode as a function of the mass corrected time of CH<sub>4</sub>, CO, CO<sub>2</sub>, H<sub>2</sub> and Ar at temperatures of 300 °C, 400 °C and 500 °C, respectively, on the H<sub>2</sub> pre-reduced Pd/γ-Al<sub>2</sub>O<sub>3</sub> catalyst. The figure shows that although the results from Figure 5 prove that the reductive H<sub>2</sub> pre-treatment led to fully reduced Pd particles on the catalyst surface prior to injecting the CH<sub>4</sub>-containing pulses, CO as well as CO<sub>2</sub> (according to reaction equation (1)) were detected as oxidation products in the outlet flow of the micro-reactor at temperatures above 300 °C. Parallel to the commencing formation of CO<sub>2</sub>, the conversion of CH<sub>4</sub> increased from approximately 58% at 300 °C to about 90% at 500 °C. These experimental findings require the ability of the Pd/y-Al<sub>2</sub>O<sub>3</sub> catalyst to supply oxidative reagents for the observed oxidation reactions, in which the activation of CH<sub>4</sub> by dissociative adsorption is considered the first step [29-31]. As the NAP-XPS measurements proved only elemental Pd<sup>0</sup> due to the reductive H<sub>2</sub> pre-treatment, only the γ-Al<sub>2</sub>O<sub>3</sub> support comes into question in this respect. Schuurman et al. [32] found that for CH<sub>4</sub> reforming with CO<sub>2</sub>, Al<sub>2</sub>O<sub>3</sub> supports this reaction via the inverse spill-over of OH-groups to the Ru active phase. Wang et al. [33] investigated the partial oxidation of CH<sub>4</sub> on a Rh/Al<sub>2</sub>O<sub>3</sub> catalyst. They observed that H<sub>2</sub>O, which was adsorbed on Al<sub>2</sub>O<sub>3</sub>, can supply O-atoms for the oxidation reaction via the inverse spill-over of H<sub>2</sub>O or OH-groups onto Rh particles. Heitnes Hofstad et al. [34] also report on spill-over processes from their supports to the Rh-active phase during the partial oxidation of CH<sub>4</sub> to syngas. These explanations, which comprise inverse spill-over processes from the support to the precious metal to help activate CH4, can be adduced to explain the enormous oxidative capability of the reductively pre-treated Pd/γ-Al<sub>2</sub>O<sub>3</sub> catalyst described in this paper, although the NAP-XPS measurements did not provide experimental evidence for the OH-groups. It could be that the concentration of OH-groups was below the detection limit of the NAP-XPS apparatus used for the experiments in Figure 4 and Figure 5.

The right-hand part of Figure 8, which displays the response pulses recorded on the H<sub>2</sub> prereduced Pd/γ-Al<sub>2</sub>O<sub>3</sub> catalyst at 500 °C, shows a very broad signal for H<sub>2</sub>. Dhainaut et al. [28] found similarly broad response pulses for H2 at 400 °C when they investigated CH4 dissociation on a pre-reduced Pd/Al<sub>2</sub>O<sub>3</sub> catalyst and ascribed it to slow H<sub>2</sub> spill-over processes from the metal to the Al<sub>2</sub>O<sub>3</sub> support. A similar process was reported by Renème et al. [35]. In their study, Cavanagh and Yates [36] investigated H<sub>2</sub> spill-over on a Rh/Al<sub>2</sub>O<sub>3</sub> catalyst whose synthesis also featured a final step of reduction with H<sub>2</sub>. They used infrared spectroscopy to examine the exchange of D<sub>2</sub> with OH-groups chemisorbed onto the Al<sub>2</sub>O<sub>3</sub> support. They conclude from their experiments that the spill-over process comprises several single steps, i.e., the fast dissociation of D<sub>2</sub> to Rh particles, the fast transition of the dissociated D-atoms to the Al<sub>2</sub>O<sub>3</sub> support, the slow migration of H-atoms across the Al<sub>2</sub>O<sub>3</sub> support and, finally, the fast replacement of H-atoms in the OH-groups by "spilled-over" D-atoms. However, on pure Al<sub>2</sub>O<sub>3</sub> without Rh loading, the exchange of H-atoms by D-atoms was not observed as the initial step, i.e., the dissociation of D<sub>2</sub> on Rh could not take place. Wang et al. [37], on the contrary, offer as an explanation for broadened H<sub>2</sub> response pulses with their Rh/Al<sub>2</sub>O<sub>3</sub> catalyst that H<sub>2</sub>O adsorbs on the Al<sub>2</sub>O<sub>3</sub> and spills over onto Rh, where it dissociates, forming H<sub>2</sub> and leaving adsorbed O-atoms and OH-groups on the metal. A different and perhaps subsidiary explanation for the broadening of the H<sub>2</sub> response pulse in Figure 8 on the righthand side at 500 °C is the slow dehydrogenation of CH<sub>4</sub>, forming H<sub>2</sub> and carbon-containing species on the catalyst surface. To shed light on the question of whether CH<sub>4</sub> dehydrogenation is relevant, the pre-reduced Pd/γ-Al<sub>2</sub>O<sub>3</sub> catalyst was titrated with a large number of pulses containing even 50% CH<sub>4</sub> in Ar. It was found that after 8250 pulses, the H<sub>2</sub> pulse responses became significantly smaller and remained constant, while in parallel the CH4 signals became much larger. Furthermore, at the end of this series, no further CO or CO<sub>2</sub> molecules could be detected in the outlet flow. This means that the catalyst lost its oxidative capability and it was concluded that only the above-mentioned dehydrogenation still took place at the end. In this respect, Figure 9 shows the averaged CO<sub>2</sub> response pulse that was detected when the CH<sub>4</sub>titrated Pd/γ-Al<sub>2</sub>O<sub>3</sub> catalyst was exposed to inlet pulses containing 50% O<sub>2</sub> in Ar at a reaction temperature of 500 °C. The detected CO<sub>2</sub> outlet intensity in Figure 9 is much higher than those that were found in the experiments outlined in Figure 8. This clearly indicates that the catalyst surface was strongly covered with carbon-containing species as a consequence of the long titration sequence and offers clear experimental evidence that CH<sub>4</sub> dehydrogenation according to reaction equation (3) is an important part of the reaction network on the prereduced Pd/γ-Al<sub>2</sub>O<sub>3</sub> catalyst at temperatures in the range of 400-500 °C. The coverage of the catalyst surface with carbon-containing substances can also explain that CH<sub>4</sub> oxidation, forming CO and CO<sub>2</sub>, was no longer possible after the titration series due to catalyst deactivation.

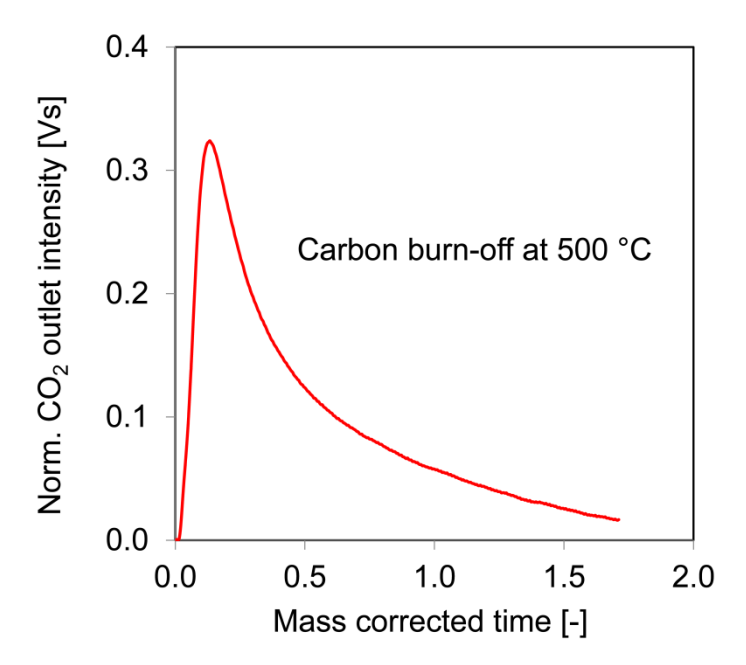


Figure 9 Outlet intensities of CO<sub>2</sub> in transient mode as a function of the mass corrected time at 500 °C after the pre-reduced Pd/ $\gamma$ -Al<sub>2</sub>O<sub>3</sub> catalyst was titrated with a mixture of 50% CH<sub>4</sub> in Ar

In order to be able to differentiate whether the delay of the H<sub>2</sub> molecules at the exit of the TAP micro-reactor associated with the broadening of the H<sub>2</sub> response pulse in Figure 8 is due to the above-described spill-over of H<sub>2</sub> from Pd to the Al<sub>2</sub>O<sub>3</sub> support or to the observed slow dehydrogenation of CH<sub>4</sub>, or even to both processes, an additional experiment was run, during which a mixture of solely 5 mole% H<sub>2</sub> in Ar was pulsed on the surface of the pre-reduced Pd/γ-Al<sub>2</sub>O<sub>3</sub> catalyst at 500 °C in transient mode. Figure 10 compares the obtained response pulses of H<sub>2</sub> and Ar with those for the CH<sub>4</sub> oxidation reaction at the same temperature of 500 °C. It can be seen that the Ar response pulses representing the diffusion-only cases through the catalyst bed were fairly comparable, with only slight differences. However, a significant broadening of the H<sub>2</sub> response pulses occurred when H<sub>2</sub> alone was pulsed on the catalyst. Thereby, no H<sub>2</sub>O formation was observed. According to the literature [28, 35, 36], this pulse shape can be ascribed to H<sub>2</sub> adsorption on the Pd and spill-over to the Al<sub>2</sub>O<sub>3</sub> support. It is interesting to note that in this figure, significant additional delay and broadening of the H<sub>2</sub> pulse response was observed in the case of the CH<sub>4</sub> oxidation reaction, which can be attributed to the slow dehydrogenation of CH<sub>4</sub> on the pre-reduced Pd/y-Al<sub>2</sub>O<sub>3</sub> catalyst at 500 °C, as was described above. This means that both processes, H<sub>2</sub> spill-over and CH<sub>4</sub> dehydrogenation, are responsible for the broad H<sub>2</sub> response pulse in Figure 8 and Figure 10.

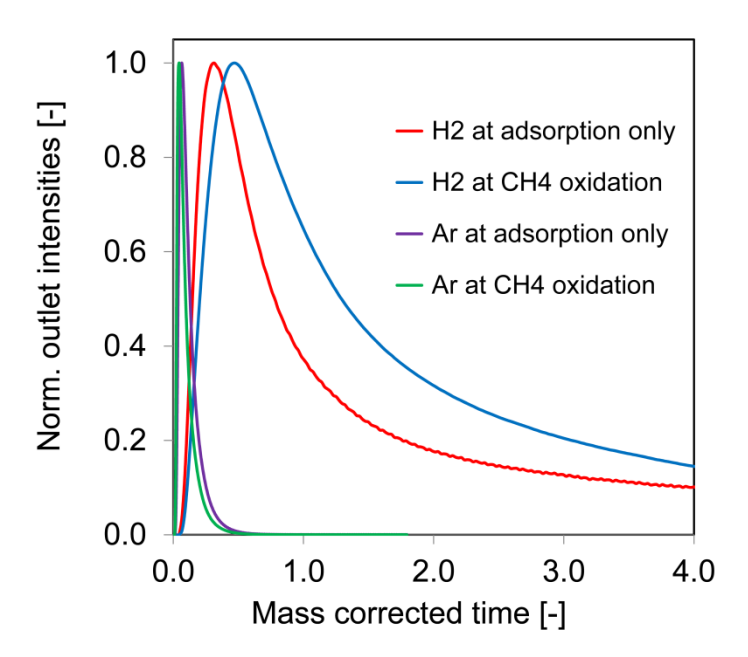


Figure 10 Outlet intensities of  $H_2$  and Ar in transient mode as a function of the mass corrected time during  $H_2$  pulsing alone and, during the  $CH_4$  oxidation reaction, with inlet pulses containing 5 mole%  $CH_4$  in Ar on the pre-reduced  $Pd/\gamma$ - $Al_2O_3$  catalyst at  $500~^{\circ}C$ 

The product formations in time at different reaction temperatures as described in Figure 7 and Figure 8 for the H<sub>2</sub> pre-reduced Pd/γ-Al<sub>2</sub>O<sub>3</sub> catalyst were similar in the cases of the pre-oxidized and CH<sub>4</sub> pre-reduced catalysts. The most apparent differences were found with respect to the formation of H<sub>2</sub>. On the CH<sub>4</sub> pre-reduced Pd/γ-Al<sub>2</sub>O<sub>3</sub> catalyst, this was more pronounced and even took place at temperatures of 400 °C and higher, while it was not observed at all at any temperature in the case of the pre-oxidized sample. It is also noteworthy that for none of the experimental series at different reaction temperatures – regardless of the catalyst pre-treatment (H<sub>2</sub> pre-reduced, CH<sub>4</sub> pre-reduced or pre-oxidized) – H<sub>2</sub>O formation was observed. Renème et al. [31] explain the lacking of H<sub>2</sub>O response pulses in their experiments by the very slow desorption of H<sub>2</sub>O and the fast re-adsorption on the Pd and/or on the Al<sub>2</sub>O<sub>3</sub> support.

Although the pre-treatment procedure did not have a decisive influence on the product formation in time, it is interesting to note whether CH<sub>4</sub> conversion was affected. In this respect, Figure 11 shows the Ar-normalized CH<sub>4</sub> outlet intensities in transient mode as a function of the mass-corrected time at different temperatures on the pre-oxidized and H<sub>2</sub> pre-reduced Pd/γ-Al<sub>2</sub>O<sub>3</sub> catalyst. As it was experimentally found that the outlet intensity of any response pulse even increases when simply the temperature in the micro-reactor rises, the CH<sub>4</sub> outlet intensities must be Ar-normalized if they are to be quantitatively compared. Ar normalization means that the recorded CH<sub>4</sub> outlet intensities at a specific temperature are multiplied by the ratio of the maximum Ar outlet intensity at the maximum reaction temperature to the Ar outlet intensity at the specific reaction temperature. This calculation guarantees that the observed differences in the CH<sub>4</sub> outlet intensities are only due to

interactions with the catalyst. Figure 11 shows that for both pre-treatments, a clear influence of the reaction temperature on the intensities of the CH<sub>4</sub> response pulses was detected. In both cases, they were highest at 100 °C and continuously decreased when the reaction temperature increased, indicating increasing CH<sub>4</sub> conversions with rising temperatures. It is interesting to note in this figure that the CH<sub>4</sub> outlet intensities on the H<sub>2</sub> pre-reduced catalyst were lower at all temperatures compared to those of the pre-oxidized catalyst. This resulted in CH<sub>4</sub> conversions of between 0-10% at low temperatures and 70-80% at high temperatures in the pre-oxidized case and between 20-30% at low temperatures and 75-90% at high temperatures in the case of pre-reduction with H<sub>2</sub>. The respective estimates for the apparent activation energies amount to  $\approx 20 \text{ kJ mole}^{-1}$  for the reductive pre-treatment with H<sub>2</sub> and  $\approx 37 \text{ kJ mole}^{-1}$ for the pre-oxidation case. These values, however, are in contrast to those found by Ciuparu et al. [3] on a Pd catalyst, which were higher in the case of pre-reductive pre-treatment. From the results of Figure 11, it can be concluded that both Pd phases, Pd<sup>0</sup> and PdO, are highly active for CH<sub>4</sub> oxidation in the absence of O<sub>2</sub> in the educt mixture, especially at reaction temperatures of between 400-500 °C. However, these data also suggest that an O<sub>2</sub>-rich Pd surface is slightly less active for CH<sub>4</sub> oxidation than a reduced Pd<sup>0</sup> phase onto whose surface OH-groups spilled over from the Al<sub>2</sub>O<sub>3</sub> support as it was described by different groups [32-34]. Maestri et al. [38] performed a micro-kinetic analysis of steam and dry reforming of CH<sub>4</sub> on Rh catalysts and conclude from their study that OH-groups are more efficient oxidizing reagents than O-atoms. However, there is no clear picture in the literature whether high O2 coverage is beneficial for the CH<sub>4</sub> oxidation reaction. Wang and Liu [39] report in their DFT study that PdO is the active phase for CH<sub>4</sub> activation on a PdO/HZSM-5 catalyst, and Maillet et al. [40] report lower apparent activation energies and higher CH<sub>4</sub> conversions on a preoxidized Pd/y-Al<sub>2</sub>O<sub>3</sub> catalyst (1 wt.% Pd). However, other groups found that the dissociative adsorption of CH4 is suppressed when the catalyst surface reveals high coverage with Oatoms [41-44].

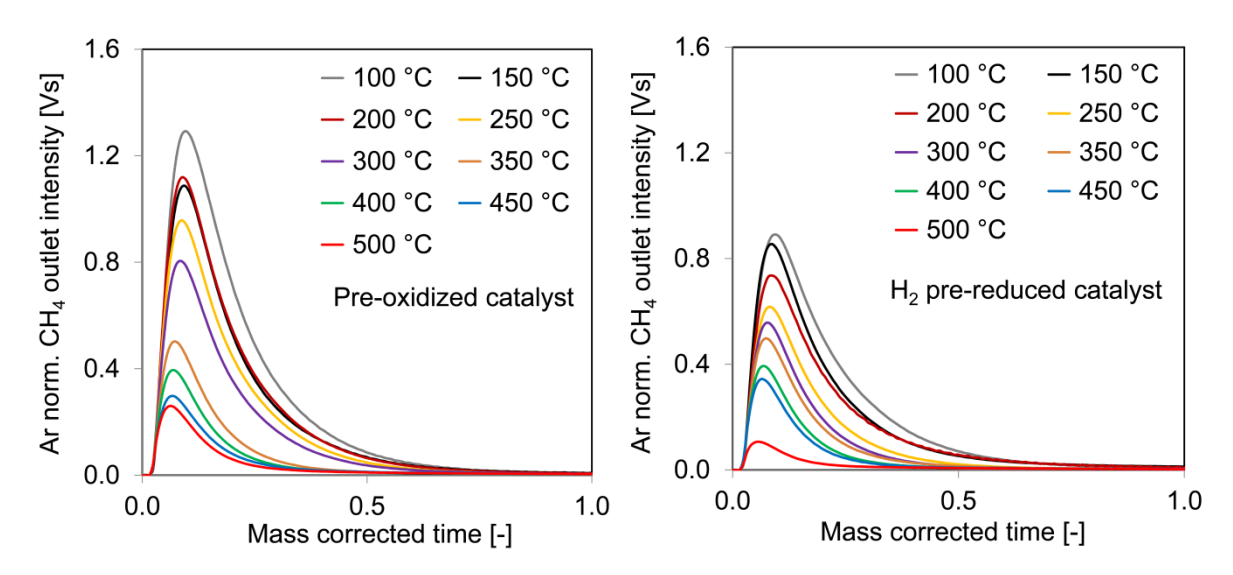


Figure 11 Ar-normalized CH<sub>4</sub> outlet intensities in transient mode as a function of the mass corrected time at different temperatures: on the pre-oxidized Pd/γ-Al<sub>2</sub>O<sub>3</sub> catalyst (left) and the H<sub>2</sub> pre-reduced Pd/γ-Al<sub>2</sub>O<sub>3</sub> catalyst (right)

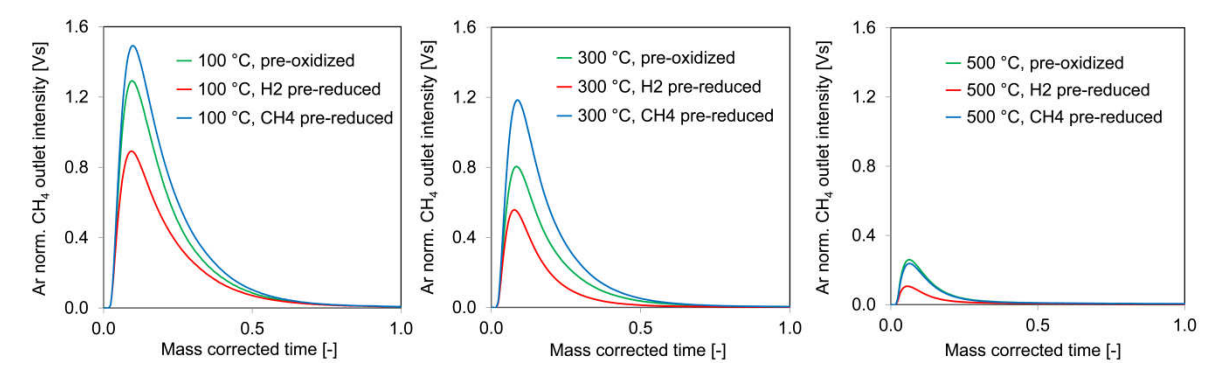


Figure 12 Ar-normalized CH<sub>4</sub> outlet intensities in transient mode as a function of the mass corrected time depending on the pre-treatment procedure of the Pd/γ-Al<sub>2</sub>O<sub>3</sub> catalyst: at 100 °C (left), 300 °C (middle) and 500 °C (right)

As a complement to Figure 11, Figure 12 shows the Ar-normalized CH4 outlet intensities in transient mode as a function of the mass corrected time depending on the pre-treatment process of the  $Pd/\gamma$ -Al<sub>2</sub>O<sub>3</sub> catalyst at 100 °C, 300 °C and 500 °C, respectively. This figure once again shows that the pre-reduction of the  $Pd/\gamma$ -Al<sub>2</sub>O<sub>3</sub> catalyst with H<sub>2</sub> led to the lowest CH4 outlet intensities and thus the highest CH4 conversions at all three reaction temperatures. The new aspect of this figure, however, is that at each reaction temperature, the CH4 outlet intensities of the CH4 pre-reduced catalyst were significantly higher than those in the case of pre-reduction with H<sub>2</sub>. The conclusions deduced from the findings in Figure 9 (coverage of the catalyst surface with carbon-containing substances after exposure to CH4 at elevated temperatures) can be transferred to explain the results in Figure 12. The pre-reduction of the  $Pd/\gamma$ -Al<sub>2</sub>O<sub>3</sub> catalyst with CH4 at 400 °C will also have led to CH4 dehydrogenation and the formation of carbon-containing deposits on the catalyst surface, which are known to reduce the catalytic activity by at least partially blocking the catalytically-active sites.

## **Conclusions**

The CH<sub>4</sub> oxidation reaction has been scientifically investigated for many years, as it is a suitable route for significantly reducing the quantities of environmentally-harmful CH<sub>4</sub> released by vehicles that run on natural gas. For the investigations reported in this paper, Pd/y-Al<sub>2</sub>O<sub>3</sub> was chosen as the catalyst, as Pd is known from the literature to be highly active when initiating CH<sub>4</sub> dissociation, which is considered the first step of CH<sub>4</sub> oxidation. NAP-XPS measurements could confirm that well-defined electronic states of the Pd phase, PdO and Pd<sup>0</sup>, were set by oxidative (flow of pure O<sub>2</sub>) and reductive (flow of H<sub>2</sub> in Ar) pre-treatments of the Pd/γ-Al<sub>2</sub>O<sub>3</sub> catalyst prior to injecting pulses of CH<sub>4</sub> onto the catalyst surface. TAP experiments revealed that both PdO and elemental Pd<sup>0</sup> were highly active for the conversion of CH<sub>4</sub>, especially at temperatures of between 400-500 °C, with CH<sub>4</sub> conversions being in the range between 70-90%. Thereby, the H<sub>2</sub> pre-reduced catalyst was even slightly more active than the pre-oxidized sample. It was concluded that the promising catalytic activity of the elemental Pd<sup>0</sup> species was only made possible by highly efficient oxidizing OH-groups that spilled over from the Al<sub>2</sub>O<sub>3</sub> support to Pd and favored the activation of the C-H bond in CH<sub>4</sub>, whereas the slightly lower catalytic activity of the PdO phase was ascribed to high coverage of the catalyst surface with O-atoms that hindered dissociative CH4 adsorption. Nevertheless, it is beneficial for the applicability of the Pd/γ-Al<sub>2</sub>O<sub>3</sub> catalyst in exhaust gas after-treatment units that it properly works under reductive and oxidative conditions. Future work will aim to further investigate the optimum ratio between PdO and Pd<sup>0</sup> and how it can be experimentally set. On the reduced surface of the Pd/γ-Al<sub>2</sub>O<sub>3</sub> catalyst, slow CH<sub>4</sub> dehydrogenation at 500 °C was observed that constitutes a possible risk of catalyst deactivation, as the catalyticallyactive sites could be blocked by carbonaceous deposits. Furthermore, the TAP experiments revealed that the reaction products CO, CO<sub>2</sub>, and H<sub>2</sub> adsorbed strongly and, to a large extent, on the catalyst surface in the whole temperature range between 100-500 °C and were, as CH<sub>4</sub>, involved in complex and reversible interactions with the catalyst surface. The role of H<sub>2</sub>O in the reaction network could not be elucidated, however, as it was not detected in the TAP experiments. Although it must have been formed, it obviously fully stuck to the Al<sub>2</sub>O<sub>3</sub> support under the TAP reaction conditions.

# Acknowledgements

The authors would like to thank the BMWi for financial support of the NAP-XPS set-up (03ET1460A).

#### References

[1] Erdgasfahrzeuge überzeugen: sauber, leise, sofort verfügbar, Deutscher Verein des Gas- und Wasserfaches e. V., 2019.

- [2] P. Lott, Methanoxidation an Edelmetallkatalysatoren zur Abgasnachbehandlung, Institut für Technische Chemie und Polymerchemie, Karlsruher Institut für Technologie, 2016.
- [3] D. Ciuparu, M.R. Lyubovski, E. Altman, L.D. Pfefferle, A. Datye, Catalytic combustion of methane over palladium-based catalysts, Catalysis Review 44 (2002) 593-649.
- [4] D. Seeburg, D.J. Liu, J. Radnik, H. Atia, M.M. Pohl, M. Schneider, A. Martin, S. Wohlrab, Structural Changes of Highly Active Pd/MeO<sub>x</sub> (Me = Fe, Co, Ni) during Catalytic Methane Combustion, Catalysts 8 (2018) 13.
- [5] M. Zanoletti, D. Klvana, J. Kirchnerova, M. Perrier, C. Guy, Auto-cyclic reactor: Design and evaluation for the removal of unburned methane from emissions of natural gas engines, Chemical Engineering Science 64 (2009) 945-954.
- [6] R. Abbasi, G. Huang, G.M. Istratescu, L. Wu, R.E. Hayes, Methane oxidation over Pt, Pt:Pd, and Pd based catalysts: Effects of pre-treatment, The Canadian Journal of Chemical Engineering 93 (2015) 1474-1482.
- [7] D. Bounechada, G. Groppi, P. Forzatti, K. Kallinen, T. Kinnunen, Effect of periodic lean/rich switch on methane conversion over a Ce–Zr promoted Pd-Rh/Al<sub>2</sub>O<sub>3</sub> catalyst in the exhausts of natural gas vehicles, Applied Catalysis B: Environmental 119-120 (2012) 91-99.
- [8] A. Tomposa, A. Tompos, J. Margitfalvi, M. Hegedus, A. Szegedi, J. Fierro, S. Rojas, Characterization of Trimetallic Pt-Pd-Au/CeO<sub>2</sub> Catalysts Combinatorial Designed for Methane Total Oxidation, Combinatorial Chemistry & High Throughput Screening 10 (2007) 71-82.
- [9] F. Huang, J. Chen, W. Hu, G. Li, Y. Wu, S. Yuan, L. Zhong, Y. Chen, Pd or PdO: Catalytic active site of methane oxidation operated close to stoichiometric air-to-fuel for natural gas vehicles, Applied Catalysis B: Environmental 219 (2017) 73-81.
- [10] N.M. Kinnunen, J.T. Hirvi, M. Suvanto, T.A. Pakkanen, Role of the Interface between Pd and PdO in Methane Dissociation, The Journal of Physical Chemistry C 115 (2011) 19197-19202.
- [11] S. Fouladvand, S. Schernich, J. Libuda, H. Grönbeck, T. Pingel, E. Olsson, M. Skoglundh, P.-A. Carlsson, Methane Oxidation Over Pd Supported on Ceria–Alumina Under Rich/Lean Cycling Conditions, Topics in Catalysis 56 (2013) 410-415.
- [12] H. Hirai, Formation and Catalytic Functionality of Synthetic Polymer-Noble Metal Colloid, Journal of Macromolecular Science: Part A Chemistry 13 (1979) 633-649.
- [13] S. Brunauer, P.H. Emmett, E. Teller, Adsorption of Gases in Multimolecular Layers, Journal of the American Chemical Society 60 (1938) 309-319.
- [14] R.W. Cranston, F.A. Inkley, 17 The Determination of Pore Structures from Nitrogen Adsorption Isotherms, in: A. Farkas, (Ed.), Advances in Catalysis, Academic Press, 1957, pp. 143-154.
- [15] NIST X-ray Photoelectron Spectroscopy Database, NIST Standard Reference Database Number 20, National Institute of Standards and Technology, Gaithersburg MD, 20899 (2000), 2000.
- [16] D. Constales, G.S. Yablonsky, L. Wang, W. Diao, V.V. Galvita, R. Fushimi, Precise non-steady-state characterization of solid active materials with no preliminary mechanistic assumptions, Catalysis Today 298 (2017) 203-208.

- [17] J.T. Gleaves, J.R. Ebner, T.C. Kuechler, Temporal Analysis of Products (TAP)—A Unique Catalyst Evaluation System with Submillisecond Time Resolution, Catalysis Reviews 30 (1988) 49-116.
- [18] J.T. Gleaves, G.S. Yablonskii, P. Phanawadee, Y. Schuurman, TAP-2: An interrogative kinetics approach, Applied Catalysis A: General 160 (1997) 55-88.
- [19] P. Phanawadee, S. O. Shekhtman, C. Jarungmanorom, G. S. Yablonsky, J. T. Gleaves, Uniformity in a thin-zone multi-pulse TAP experiment: numerical analysis, Chemical Engineering Science 58 (2003) 2215-2227.
- [20] S.O. Shekhtman, G.S. Yablonsky, J.T. Gleaves, R. Fushimi, "State defining" experiment in chemical kinetics—primary characterization of catalyst activity in a TAP experiment, Chemical Engineering Science 58 (2003) 4843-4859.
- [21] S.O. Shekhtman, G.S. Yablonsky, J.T. Gleaves, R.R. Fushimi, Thin-zone TAP reactor as a basis of "state-by-state transient screening", Chemical Engineering Science 59 (2004) 5493-5500.
- [22] M.C. Militello, S.J. Simko, Elemental Palladium by XPS, Surface Science Spectra 3 (1994) 387-394.
- [23] T.J. Sarapatka, Palladium-induced charge transports with palladium/alumina/aluminum interface formation, The Journal of Physical Chemistry 97 (1993) 11274-11277.
- [24] J.F. Moulder, W.F. Stickle, P.E. Sobol, K.D. Bomben, Handbook of X-ray Photoelectron Spectroscopy, Physical Electronics Inc., Eden Prairie, MN, 1995.
- [25] M. Brun, A. Berthet, J.C. Bertolini, XPS, AES and Auger parameter of Pd and PdO, Journal of Electron Spectroscopy and Related Phenomena 104 (1999) 55-60.
- [26] M.C. Militello, S.J. Simko, Palladium Oxide (PdO) by XPS, Surface Science Spectra 3 (1994) 395-401.
- [27] W.K. Kuhn, J. Szanyi, D.W. Goodman, CO adsorption on Pd(111): the effects of temperature and pressure, Surface Science 274 (1992) L611-L618.
- [28] F. Dhainaut, A.C. van Veen, S. Pietrzyk, P. Granger, CH<sub>4</sub> Dissociation Mechanisms on Aged Three-Way Natural Gas Vehicle Pd/Al<sub>2</sub>O<sub>3</sub> Catalyst, Topics in Catalysis 60 (2016) 295-299.
- [29] A. Hellman, A. Resta, N.M. Martin, J. Gustafson, A. Trinchero, P.A. Carlsson, O. Balmes, R. Felici, R. van Rijn, J.W. Frenken, J.N. Andersen, E. Lundgren, H. Gronbeck, The Active Phase of Palladium during Methane Oxidation, The Journal of Physical Chemistry Letters 3 (2012) 678-682.
- [30] F. Dhainaut, P. Granger, Kinetic Modeling of the Metal/Support Interaction for CH<sub>4</sub> Reaction over Oxidized Pd/Al<sub>2</sub>O<sub>3</sub>, Topics in Catalysis (2018).
- [31] Y. Renème, S. Pietrzyk, F. Dhainaut, M. Chaar, A.C. van Veen, P. Granger, Reaction Pathways Involved in CH<sub>4</sub> Conversion on Pd/Al<sub>2</sub>O<sub>3</sub> Catalysts: TAP as a Powerful Tool for the Elucidation of the Effective Role of the Metal/Support Interface, Front Chem 4 (2016) 7.
- [32] Y. Schuurman, C. Marquez-Alvarez, V.C.H. Kroll, C. Mirodatos, Unraveling mechanistic features for the methane reforming by carbon dioxide over different metals and supports by TAP experiments Catalysis Today 46 (1998) 185-192.

- [33] D. Wang, O. Dewaele, A.M.D. Groote, G.F. Froment, Reaction Mechanism and Role of the Support in the Partial Oxidation of Methane on Rh/Al<sub>2</sub>O<sub>3</sub>, Journal of Catalysis 159 (1996) 418-426.
- [34] K. Heitnes Hofstad, J.H.B.J. Hoebink, A. Holmen, G.B. Marin, Partial oxidation of methane to synthesis gas over rhodium catalysts, Catalysis Today 40 (1998) 157-170.
- [35] Y. Renème, F. Dhainaut, Y. Schuurman, C. Mirodatos, P. Granger, Comparative surface analysis and TAP measurements to probe the NO adsorptive properties of natural gas vehicle Pd–Rh/Al<sub>2</sub>O<sub>3</sub> catalyst, Applied Catalysis B: Environmental 160-161 (2014) 390-399.
- [36] R.R. Cavanagh, J.T. Yates, Hydrogen spillover on alumina—A study by infrared spectroscopy, Journal of Catalysis 68 (1981) 22-26.
- [37] D. Wang, O. Dewaele, G.F. Froment, Methane adsorption on Rh/Al<sub>2</sub>O<sub>3</sub>, Journal of Molecular Catalysis A: Chemical 136 (1998) 301-309.
- [38] M. Maestri, D.G. Vlachos, A. Beretta, G. Groppi, E. Tronconi, Steam and dry reforming of methane on Rh: Microkinetic analysis and hierarchy of kinetic models, Journal of Catalysis 259 (2008) 211-222.
- [39] J.-g. Wang, C.-j. Liu, Density functional theory study of methane activation over PdO/HZSM-5, Journal of Molecular Catalysis A: Chemical 247 (2006) 199-205.
- [40] T. Maillet, C. Solleau, J. Barbier Jr., D. Duprez, Oxidation of carbon monoxide, propene, propane and methane over a Pd/Al<sub>2</sub>0<sub>3</sub> catalyst. Effect of the chemical state of Pd, Applied Catalysis B: Environmental 14 (1997) 85-95.
- [41] E. Becker, P.-A. Carlsson, H. Grönbeck, M. Skoglundh, Methane oxidation over alumina supported platinum investigated by time-resolved in situ XANES spectroscopy, Journal of Catalysis 252 (2007) 11-17.
- [42] M. Valden, J. Pere, M. Hirsimäki, S. Suhonen, M. Pessa, Activated adsorption of methane on clean and oxygen-modified Pt{111} and Pd{110}, Surface Science 377-379 (1997) 605-609.
- [43] M. Valden, J. Pere, N. Xiang, M. Pessa, Influence of preadsorbed oxygen on activated chemisorption of methane on Pd(110), Chemical Physics Letters 257 (1996) 289-296.
- [44] Z. Li, G.B. Hoflund, A Review on Complete Oxidation of Methane at Low Temperatures, Journal of Natural Gas Chemistry 12 (2003) 153-160.